

UCLA
COMPUTATIONAL AND APPLIED MATHEMATICS

Solitary-Wave Solutions of the Benjamin Equation

John P. Albert
Jerry L. Bona
Juan Mario Restrepo

May 1997
CAM Report 97-23

Department of Mathematics
University of California, Los Angeles
Los Angeles, CA. 90024-1555

SOLITARY-WAVE SOLUTIONS OF THE BENJAMIN EQUATION*

JOHN P. ALBERT[†] JERRY L. BONA[‡] AND JUAN MARIO RESTREPO[§]

Abstract. Considered here is a model equation put forward by Benjamin that governs approximately the evolution of waves on the interface of a two-fluid system in which surface tension effects cannot be ignored. Our principal focus is the traveling-wave solutions called solitary waves, and three aspects will be investigated. A constructive proof of the existence of these waves together with a proof of their stability is developed. Continuation methods are used to generate a scheme capable of numerically approximating these solitary waves. The computer-generated approximations reveal detailed aspects of the structure of these waves. They are symmetric about their crests, but unlike the classical Korteweg-de Vries solitary waves, they feature a finite number of oscillations. The derivation of the equation is also revisited to get an idea of whether or not these oscillatory waves might actually occur in a natural setting.

Key words. Benjamin equation, solitary waves, oscillatory solitary waves, stability, continuation methods

AMS subject classifications. Primary 76B25; Secondary 35Q51, 35Q35, 65H20, 58G16

1 INTRODUCTION

This paper was inspired by recent work of Benjamin ([7], [8]) concerning waves on the interface of a two-fluid system. Benjamin was concerned with an incompressible system that, at rest, consists of a layer of depth h_1 of light fluid of density ρ_1 bounded above by a rigid plane and resting upon a layer of heavier fluid of density $\rho_2 > \rho_1$ of depth h_2 , also resting on a rigid plane. Because of the density difference, waves can propagate along the interface between the two fluids. In Benjamin's theory, diffusivity is ignored, but the parameters of the system are such that capillarity cannot be discarded.

Benjamin focused attention upon waves that do not vary with the coordinate perpendicular to the principal direction of propagation. The waves in question are thus assumed to propagate in only one direction, the positive x direction, say, and to have long wavelength λ and small amplitude a relative to h_1 . The small parameters $\epsilon = \frac{a}{h_1}$ and $\mu = \frac{h_2}{\lambda}$ are supposed to be of the same order of magnitude, so that nonlinear and dispersive effects are balanced. Furthermore, the lower layer is assumed to be very deep relative to the upper layer, so that $\delta = \frac{h_2}{h_1}$ is large.

The coordinate system is chosen so that, at rest, the interface is located at $z = 0$. Thus, the upper bounding plane is located at $z = h_1$ and the lower plane at $z = -h_2$. Let $\eta(x, t)$ denote the downward vertical displacement of the interface from its rest

* Work supported in part by the Mathematical, Information, and Computational Sciences Division subprogram of the Office of Computational and Technology Research, U.S. Department of Energy, under Contract W-31-109-Eng-38. JLB was supported by NSF and Keck Foundation grants. JMR was supported by an appointment to the Distinguished Postdoctoral Research Program sponsored by the U.S. Department of Energy, Office of University and Science Education Programs, and administered by the Oak Ridge Institute for Science and Education.

[†]Mathematics Department, University of Oklahoma Norman OK, 73019 U.S.A. (jalbert@uoknor.edu)

[‡]Mathematics Department and Texas Institute for Computational and Applied Mathematics, University of Texas at Austin, Austin TX, 78712 U.S.A. (bona@math.utexas.edu)

[§]Mathematics Department, University of California, Los Angeles Los Angeles, CA 90095 U.S.A. (restrepo@math.ucla.edu)

position at the horizontal coordinate x at time t (so that positive values of η correspond to depressions of the interface). When the variables are suitably non-dimensionalized (see Section 2 below), the equation derived by Benjamin takes the form

$$(1) \quad \eta_t + c_0(\eta_x + 2r\eta\eta_x - \alpha L\eta_x - \beta\eta_{xxx}) = 0,$$

where the subscripts denote partial differentiation. The coefficients in (1) are given by

$$c_0 = \sqrt{\frac{\rho_2 - \rho_1}{\rho_1}}, \quad r = \frac{3a}{4h_1},$$

$$\alpha = \frac{h_1\rho_2}{2\lambda\rho_1}, \quad \beta = \frac{T}{2g\lambda^2(\rho_2 - \rho_1)},$$

where T is the interfacial surface tension and g is the gravity constant. The operator $L = H\partial_x$ is the composition of the Hilbert transform H and the spatial derivative. A Fourier multiplier operator with symbol $|k|$, L first arose in the context of nonlinear, dispersive wave propagation in the studies [5] and [16] on internal waves in deep water (see also [24]).

Benjamin pointed out that the functionals

$$F(\eta) = \int_{-\infty}^{\infty} \frac{1}{2}\eta^2 dx \quad \text{and} \quad G(\eta) = \int_{-\infty}^{\infty} \left[\frac{1}{3}r\eta^3 - \frac{1}{2}\alpha\eta L\eta + \frac{1}{2}\beta\eta_x^2 \right] dx$$

are constants of the motion for Eq. (1); that is, if η is a smooth solution of Eq. (1) that vanishes suitably at $x = \pm\infty$, then $F(\eta)$ and $G(\eta)$ are independent of t , being determined by their initial values at $t = 0$, say. Note that $F + G$ is a Hamiltonian for Eq. (1).

For $\alpha = 0$, Eq. (1) has the form of the Korteweg-de Vries equation (KdV equation henceforth), while for $\beta = 0$, the form is that of the Benjamin-Ono equation. In fact, the signs of the third and fourth terms on the left-hand side of Eq. (1) are such that the KdV-type dispersion relation arising from the fourth term competes against the Benjamin-Ono-type dispersion relation arising from the third term. To see this more clearly, consider the linearized initial-value problem

$$(2) \quad \begin{aligned} \eta_t + c_0(\eta_x - \alpha L\eta_x - \beta\eta_{xxx}) &= 0, \\ \eta(x, 0) &= f(x), \end{aligned}$$

posed for $x \in \mathbb{R}$ and $t \geq 0$. The formal solution of Eq. (2) is

$$\eta(x, t) = \frac{1}{2\pi} \int_{-\infty}^{\infty} e^{ik(x - c_B(k)t)} \hat{f}(k) dk,$$

where \hat{f} denotes the Fourier transform of f and the function $c_B(k)$, known as the dispersion relation for Eq. (2), is given by

$$(3) \quad c_B(k) = c_B(k; \alpha, \beta) = c_0(1 - \alpha|k| + \beta k^2).$$

The KdV dispersion term βk^2 and the Benjamin-Ono dispersion term $\alpha|k|$ have opposite signs in Eq. (3), and are comparable in size when $|k|$ is near $k_m = \alpha/2\beta$, the value of $|k|$ at which c_B takes its minimum $c_m = c_0(1 - \alpha^2/4\beta)$. Figure 1 shows the behavior of $c_B(k)$ near $k = 0$ for various values of α when $\beta = 2$ and $c_0 = 1$.

Notice that the dispersion relation has a discontinuous first derivative at $k = 0$ for $\alpha > 0$, and that the value of c_m will be positive as long as $\alpha^2/4\beta < 1$. According

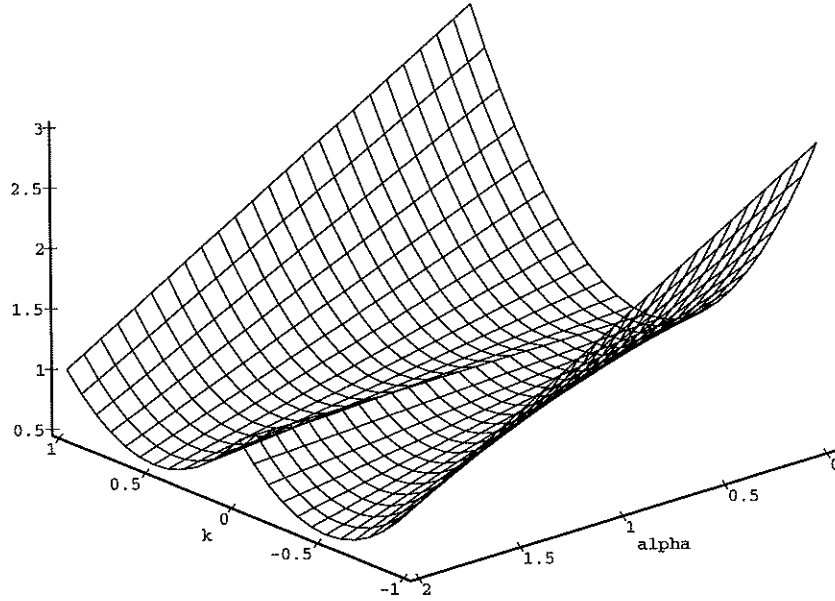


FIGURE 1. Dispersion relation $c_B(k; \alpha, \beta)$ with $\beta = 2.0$.

to Benjamin's commentary, Eq. (1) should be physically relevant when $\alpha^2/4\beta$ is comparable in size to μ , so that $(c_0 - c_m)/c_0$ is comparable to μ , and k_m is comparable to μ/α which is of order 1. It follows that for values of k near k_m the contributions of the KdV and Benjamin-Ono terms to the dispersion relation are of similar magnitude and are oppositely directed. The question of the relative sizes of these two dispersive terms will be discussed at more length in Section 2.

In this paper, attention is focused on solitary-wave solutions of Eq. (1), which are solutions of the form

$$\eta(x, t) = \Phi(x - c_0(1 - C)t),$$

where $\Phi(X)$ and its derivatives tend to zero as the variable $X = x - c_0(1 - C)t$ approaches $\pm\infty$. The dimensionless variable C represents the relative decrease in the speed of the solitary wave from the speed c_0 of very long-wavelength solutions of the linearized Eq. (2). Substituting this form for η into Eq. (1) and integrating once with respect to X yields the equation

$$C\Phi - \alpha L\Phi - \beta\Phi'' + r\Phi^2 = 0,$$

which, after transforming the dependent variable to

$$(4) \quad \phi(X) = \frac{-r}{C}\Phi\left(\sqrt{\frac{\beta}{C}}X\right),$$

can be rewritten as

$$(5) \quad Q(\phi, \gamma) \equiv \phi - 2\gamma L\phi - \phi'' - \phi^2 = 0,$$

where

$$\gamma = \frac{\alpha}{2\sqrt{\beta C}}.$$

Thus, possible solitary-wave solutions of Eq. (1) are solutions of the family of equations Eq. (5), indexed by the parameter γ . Since the assumptions underlying the derivation of Eq. (1) imply that C is a small number, of size comparable to $(c_0 - c_m)/c_0 \sim \mu \sim \alpha^2/4\beta$, it follows that in the regime of physical parameters for which Benjamin's equation is relevant, γ should be an order-one quantity.

The questions of existence, asymptotics, and stability of solitary-wave solutions of (1) were studied by Benjamin in [7] and [8]. Using the degree-theoretic approach of [9], he showed that for each value of γ in the range $[0, 1)$, Eq. (5) has a solution $\phi = \phi_\gamma$ which is an even function of X with

$$\phi_\gamma(0) = \max_{X \in \mathbb{R}} \phi_\gamma(X) > 0.$$

Notice that, according to the transformation in Eq. (4), such a ϕ_γ corresponds to a wave motion for which the interface is deflected upwards at the point of maximum deflection. In this respect, the solitary-wave solutions of Eq. (5) differ from Benjamin-Ono-type solitary waves, which in the fluid system considered here would correspond to downward deflections of the interface. Also, the condition $0 < \gamma < 1$ means that the dimensional wave speed of the solitary wave lies in the range $-\infty < c_0(1 - C) < c_m$. In particular, values of γ near zero correspond to large negative wave speeds, and thus to solutions of questionable physical relevance.

Benjamin also provided some formal asymptotics suggesting that, for each fixed value of γ , there is a bounded range of values of X in which the solitary wave $\phi_\gamma(X)$ will oscillate between positive and negative values, and that outside this bounded region, $|\phi_\gamma(X)|$ should decay monotonically like $1/|X|^2$. Finally, he sketched a perturbation-theoretic approach to a proof of existence of a branch of solutions of Eq. (5), defined for γ near 0, which correspond to stable solutions of the initial-value problem for Eq. (1).

The plan of this paper is as follows. In Section 2 we determine more precisely the range of parameters for which Eq. (1) is a good approximation to the more general equations from which it was derived. This aspect bears crucially on whether these waves are realizable in the laboratory or can be expected to occur in nature. In Section 3, we present a complete theory of existence and stability of solitary-wave solutions corresponding to values of γ near 0; in fact this result will appear as a special case of a general result on perturbations of solitary-wave solutions of nonlinear dispersive wave equations. Our argument is based on the Implicit Function Theorem, and yields an analytic dependence of solitary waves on the parameter γ . Section 4 is devoted to explaining an algorithm for the approximation of solitary-wave solutions. The algorithm is a continuation method based on the Contraction Mapping Principle that underlies the proof of existence made via the Implicit Function Theorem. We then present some numerical approximations of solitary-wave solutions of Benjamin's equation using a computer code based on this algorithm. The output graphically reveals aspects of the structure of the solitary-wave solutions of Eq. (1). The paper concludes with a summary and further discussion in Section 5.

2 PHYSICAL REGIME OF VALIDITY OF BENJAMIN'S EQUATION

In this section we examine the conditions under which the dispersion relation appearing in Benjamin's equation is a valid approximation to the dispersion relation induced by a more general system of equations for internal waves in a two-fluid system. Some general conclusions are drawn as to the types of fluids and configurations for which Benjamin's equation may be relevant as a model, and for which solitary waves of the type considered in Sections 3 and 4 below might be observed.

Consider two incompressible fluids, each of constant density, contained between rigid horizontal planes, with the lighter of the two fluids resting in a layer of nearly uniform depth atop a layer of the heavier fluid, also nearly uniform in depth. Ideally, the fluids are non-dissipative, but for real fluids we require that the Reynolds number induced by the dynamics under consideration be large. We also ignore possible diffusive effects across the interface that would lead to nonhomogeneous layers. It is assumed that the balance of pressure on either side of the interface is proportional to the curvature of the interface. The only external force acting upon the system is that of gravity. The flow is assumed to be irrotational (within each of the layers of fluid) and is two-dimensional in the sense that the flow variables depend only on a horizontal coordinate x , the vertical coordinate z , and the time variable t .

The equations that govern the dynamics of the two-fluid system just described are well known (see [19] and references contained therein). In the interior of each fluid layer, the laws of conservation of mass and momentum imply the equations

$$\phi_{ixx} + \phi_{izz} = 0 \quad (i = 1, 2)$$

and

$$\rho_i \left[\phi_{it} + \frac{1}{2}(\phi_{ix})^2 + \frac{1}{2}(\phi_{iz})^2 + gz \right] = -p_i \quad (i = 1, 2).$$

Here g is the gravitational acceleration; $i = 1$ connotes the upper layer and $i = 2$ the lower layer; and the fluid variables within each layer are the velocity potentials $\phi_i(x, z, t)$, the pressures $p_i(x, z, t)$, and the densities ρ_i . The boundary planes, which are located at $z = h_1$ and $z = -h_2$, are rigid and impermeable, so that

$$\phi_{1z} = 0 \quad \text{at } z = h_1$$

and

$$\phi_{2z} = 0 \quad \text{at } z = -h_2.$$

At the interface $z = \eta(x, t)$ (which is located at $z = 0$ when the system is undisturbed), one has the kinematic conditions

$$\eta_t - \phi_{iz} + \phi_{ix}\eta_x = 0 \quad (i = 1, 2)$$

and

$$p_2 - p_1 = -T\eta_{xx},$$

where T denotes the interfacial surface tension. In the latter equation, η_{xx} is a good approximation to the curvature of the interface provided the slope η_x is small.

As in Section 1, we assume that $\epsilon = a/h_1$ and $\mu = h_1/\lambda$ are small, where a is a typical amplitude and λ a typical wavelength of the interfacial waves being modeled. To make explicit the effects of this assumption, we non-dimensionalize the variables in the above equations, so that the rescaled variables and their derivatives have values

on the order of unity, and small terms will be identified by the presence of factors of ϵ or μ . The rescaled independent variables (marked by tildes) are

$$\tilde{x} = \frac{x}{\lambda}, \quad \tilde{t} = \frac{vt}{\lambda}, \quad \tilde{z}_1 = \frac{z}{h_1}, \quad \tilde{z}_2 = \frac{z}{h_2},$$

where v denotes $\sqrt{gh_1}$ and z is rescaled to \tilde{z}_1 at points above the interface and to \tilde{z}_2 at points below the interface. The dependent variables are rescaled as

$$\tilde{p}_i = \frac{p_i}{\rho_2 v^2}, \quad \tilde{\eta} = \frac{\eta}{a}, \quad \tilde{\phi}_i = \frac{v\phi_i}{g\lambda a}.$$

In the non-dimensionalized variables (from which the tildes will henceforth be dropped for ease of reading), the equations of motion may be written as

$$\begin{aligned} \mu^2 \phi_{1xx} + \phi_{1z_1 z_1} &= 0 && \text{for } z_1 > \epsilon\eta; \\ \mu^2 \delta^2 \phi_{2xx} + \phi_{2z_2 z_2} &= 0 && \text{for } z_2 < \epsilon\eta/\delta; \\ \epsilon \phi_{1t} + \frac{1}{2} \epsilon^2 \phi_{1x}^2 + \frac{1}{2} \frac{\epsilon^2}{\mu^2} \phi_{1z_1}^2 + z_1 &= -(1 + \tau)p_1 && \text{for } z_1 > \epsilon\eta; \\ \epsilon \phi_{2t} + \frac{1}{2} \epsilon^2 \phi_{2x}^2 + \frac{1}{2} \frac{\epsilon^2}{\mu^2 \delta^2} \phi_{2z_2}^2 + \delta z_2 &= -p_2 && \text{for } z_2 < \epsilon\eta/\delta; \\ \eta_t + \epsilon \phi_{1x} \eta_x - \frac{1}{\mu^2} \phi_{1z_1} &= 0 && \text{at } z_1 = \epsilon\eta; \\ \eta_t + \epsilon \phi_{2x} \eta_x - \frac{1}{\mu^2 \delta} \phi_{2z_2} &= 0 && \text{at } z_2 = \epsilon\eta/\delta; \\ \mu(1 + \tau)(p_2 - p_1) + \sigma \tau \epsilon \eta_{xx} &= 0 && \text{at } z_1 = \epsilon\eta \text{ and } z_2 = \epsilon\eta/\delta; \\ \phi_{1z_1} &= 0 && \text{at } z_1 = 1; \\ \phi_{2z_2} &= 0 && \text{at } z_2 = -1; \end{aligned}$$

where $\delta = h_2/h_1$, and σ and τ are dimensionless quantities defined by

$$\sigma = \frac{T}{(\rho_2 - \rho_1)g\lambda^2}$$

and

$$\tau = (\rho_2/\rho_1) - 1.$$

Note that σ and τ represent the only influence of the physical properties of the fluids on the system. (Since $\rho_2 > \rho_1$, both σ and τ must be positive.)

If the preceding system is linearized by omitting terms of higher order in ϵ , the resulting equations will have sinusoidal solutions of the form

$$\begin{aligned} \phi_i(x, z_i, t) &= A_i(k, z_i) e^{ik(x-ct)} \quad (i = 1, 2), \\ p_i(x, z_i, t) &= B_i(k, z_i) e^{ik(x-ct)} \quad (i = 1, 2), \\ \eta(x, t) &= C(k) e^{ik(x-ct)}, \end{aligned}$$

where k is an arbitrary real number. The linearized equations determine not only the forms of the functions A_i , B_i , and C , but also the dispersion relation

$$c^2(k) = \frac{\tau(1 + k^2\sigma)}{(1 + \tau)\mu k \coth(\mu\delta k) + \mu k \coth(\mu k)}.$$

To obtain conditions for the validity of Benjamin's equation, we now determine when the function $c(k)$ may be approximated by a function of the form appearing in Eq. (3) above.

When $\theta \equiv \mu\delta$ is large enough that $\coth(\theta) \approx 1$, and $|k|$ is not too small, the function $c^2(k)$ is approximately equal to

$$(7) \quad c_a^2(k) = \frac{\tau(1+k^2\sigma)}{(1+\tau)\mu|k| + \mu k \coth(\mu k)}.$$

An expansion of the right-hand side of Eq. (7) with respect to the small parameter μ yields

$$c_a(k) = \sqrt{\tau} (1 + \sigma k^2)^{1/2} \left[1 - \frac{1}{2}(1+\tau)|k|\mu + \left(\frac{3}{8}(1+\tau)^2 - \frac{1}{6} \right) k^2 \mu^2 + O(\mu^3) \right].$$

The approximation which results in the Benjamin equation now proceeds on the assumption that σ is small. Indeed, σ and τ are related to the parameters α and β introduced in Section 1 by

$$\alpha = \frac{\mu(1+\tau)}{2} \quad \text{and} \quad \beta = \frac{\sigma}{2};$$

and therefore, if τ is not too large, Benjamin's assumption that $\alpha^2/4\beta = O(\mu)$ corresponds to the assumption that $\sigma = O(\mu)$. For the moment, however, we simply treat σ as a small parameter without comparing its size to that of μ . Then an expansion of $c_a(k)$ through quadratic order in both μ and σ yields the expression

$$(8) \quad c_a(k) = \sqrt{\tau} \left[1 - \frac{1}{2}(1+\tau)|k|\mu + \frac{1}{2}k^2\sigma + \left(\frac{3}{8}(1+\tau)^2 - \frac{1}{6} \right) k^2\mu^2 - \frac{1}{4}(1+\tau)k^2|k|\mu\sigma - \frac{1}{8}k^4\sigma^2 + O(\mu^3, \mu^2\sigma, \mu\sigma^2, \sigma^3) \right].$$

(A minor error in Eq. (2.2) of [7] has been corrected here.)

In the present scaling, the wavenumbers k of interest will have absolute values on the order of unity. Therefore the terms on the right-hand side of Eq. (8) can be ordered according to the size of the numbers $(1+\tau)\mu$ and σ . One way to arrive at an approximate dispersion relation of the form appearing in Eq. (3) is to assume that

$$(9) \quad (1+\tau)^2\mu^2 \ll \sigma.$$

Then, to first order in $(1+\tau)\mu$, the function $c_a(k)$ can be approximated by

$$c_b(k) = \sqrt{\tau} \left[1 - \frac{1}{2}(1+\tau)|k|\mu + \frac{1}{2}k^2\sigma \right],$$

which is the same form as that obtained by Benjamin.

To verify the validity of the above formal arguments, and to obtain an idea of the sizes of the error terms in the approximations, the relative error

$$\frac{c_b(k) - c(k)}{c(k)}$$

was plotted against k for various values of the parameters δ , μ , σ and τ . A typical plot is shown in Figure 2a, where k and σ vary over the ranges $-1 \leq k \leq 1$ and $0 \leq \sigma \leq 1.25$, while $\delta = 100$, $\tau = 0.5$, and $\mu = 0.05$ are held constant. The relative

error is small for small values of σ , and stays below 10% even for values of σ up to unity. The ridge down the middle of the surface, which persists up to the point where $\sigma = 0$ and $k = 0$, is due to the error of replacing $\coth(\theta k)$ by $\operatorname{sgn} k$, which was made in passing from $c(k)$ to the approximation $c_a(k)$ in Eq. (7). Here $\theta = 5$, and $\coth(\theta k)$ will not be close to $\operatorname{sgn} k$ for $|k|$ less than about 0.5; yet the overall approximation remains accurate. As can be seen from Figure 2b, even reducing θ to $\theta = 1.5$ only slightly magnifies the error. In Figure 2c, μ varies over the range $0 \leq \mu \leq 0.5$ while $\sigma = 0.01$, $\tau = 0.5$, and $\theta = 5$ are held constant. Comparison with Figure 2a shows that the relative error is more sensitive to μ than it is to σ , although it is within a reasonable range for μ between 0 and 0.25. Finally, Figure 2d (in which $\delta = 100$, $\sigma = 0.01$, and $\mu = 0.05$ are held constant) shows that the relative error increases only slowly with τ in the range $0 \leq \tau \leq 1$ and beyond. In general, $c_b(k)$ will be a good approximation to $c(k)$ over the range $|k| \leq 1$ provided μ and σ are small, θ is not too small, and τ is not too large. When $\theta \geq 5$ and $\tau \leq 0.5$, for example, the relative error of the approximation is less than 1% for $0 \leq \mu \leq 0.5$ and $0 \leq \sigma \leq 0.25$.

The computations just described show that condition (9) is not necessary for the validity of Benjamin's approximation to the dispersion relation. However, when (9) is violated, σ is small enough that the contribution of the term $\frac{1}{2}k^2\sigma$ to the right-hand side of $c_b(k)$ is no more significant than the contribution of the $O((1+\tau)^2\mu^2)$ term in Eq. (8), so that the Benjamin dispersion relation is no better an approximation of $c(k)$ than is the Benjamin-Ono dispersion relation

$$c_{BO}(k) = \sqrt{\tau} \left[1 - \frac{1}{2}(1+\tau)|k|\mu \right].$$

Furthermore, if (9) is violated, then the solitary-wave parameter

$$\gamma = \frac{\alpha}{2\sqrt{\beta C}} = \frac{(1+\tau)\mu}{\sqrt{8\sigma C}}$$

will not be less than 1 unless C is on the order of unity or greater. The condition $\gamma < 1$ is necessary for the existence of the solitary waves studied below in Sections 3 and 4. But, as mentioned in Section 1, solitary-wave solutions of physical interest should correspond to values of C on the order of μ , or in other words to values of C much less than unity. Therefore (9) is a necessary condition for the physical relevance of the solitary-wave solutions considered in Sections 3 and 4.

To summarize the foregoing, c_b is a good approximation to c when $\theta \geq \theta_0 \approx 2$, $\tau \leq \tau_0 \approx 5$, $\mu \ll 1$, and $\sigma \ll 1$. Furthermore, if solitary waves of the type studied below in Sections 3 and 4 are to exist and be consistent with the assumptions made in deriving the Benjamin equation, then condition (9) should also be satisfied.

The requirement that $\mu \ll 1$ means that $h_1/\lambda \ll 1$. In a laboratory setting this could be achieved either by making the upper layer very thin or by creating waves with long length scales. If h_1 is small, however, then the Reynolds number $R = vh_1/\nu$ (in which $v = \sqrt{gh_1}$ and ν is a measure of a mechanism such as dynamic viscosity which attenuates the waves) will not be large. Hence attenuation will play a significant role in the dynamics of the system, and the inviscid equation (1) will not be an accurate model even on short time scales. Thus in a laboratory experiment for testing the predictions of Eq. (1), the upper layer should not be made extremely thin, and disturbances with long wavelengths relative to the upper layer should be created. On the other hand, the requirements that $\mu \ll 1$ and $\theta = \mu\delta \geq \theta_0$ combine to imply that $\frac{h_2}{h_1} \geq \theta_0/\mu \gg 1$, so that the lower layer will have to be fairly deep.

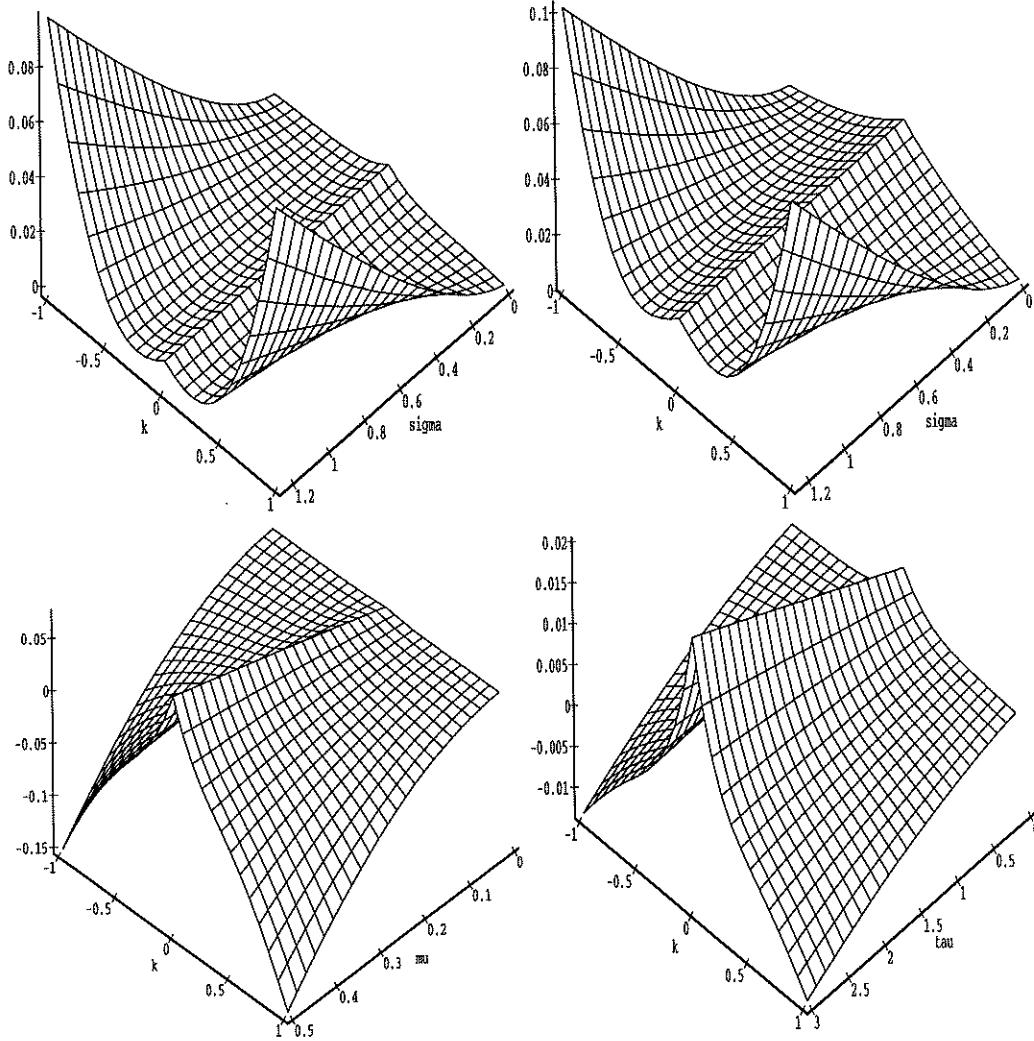


FIGURE 2. The relative error $\frac{c_b - c}{c}$, for (a) $\mu = 0.05$, $\tau = 0.5$, $\theta = 5$; (b) $\mu = 0.05$, $\tau = 0.5$, $\theta = 1.5$; (c) $\sigma = 0.01$, $\tau = 0.5$, $\theta = 5$; (d) $\mu = 0.05$, $\sigma = 0.01$, $\theta = 5$.

The requirement $\sigma \ll 1$, or in other words,

$$\frac{T}{(\rho_2 - \rho_1)g\lambda^2} \ll 1,$$

is satisfied in any configuration of two fluids if the waves under consideration are long enough so that λ is sufficiently large. The requirement in condition (9), on the other hand, strongly restricts the allowable configurations of the system. Writing (9) as

$$h_1 \ll \left(\frac{\rho_1}{\rho_2}\right) \sqrt{\frac{T}{g(\rho_2 - \rho_1)}},$$

we see that if the condition is to be satisfied for fluid depths h_1 that are not too small then the density difference $\rho_2 - \rho_1$ must be small and the interfacial surface tension T must be large. If for example $T = 80$ dyne/cm and h_1 is to be greater than 1 cm,

then (9) will hold only if $\rho_2 - \rho_1$ is significantly less than 0.08.

3 EXISTENCE AND STABILITY OF SOLITARY-WAVE SOLUTIONS

At issue in this section is the mathematical question of existence of solitary-wave solutions $\eta(x, t) = \Phi(x - c_0(1 - C)t)$ of Eq. (1) for small values of the parameter $\gamma = \alpha/(2\sqrt{\beta C})$. If these waves exist, their physical relevance comes into question, and thus their stability is also within the purview of an initial inquiry. For $\gamma = 0$, existence is provided by the exact formula

$$\eta(x, t) = -\frac{3C}{r} \operatorname{sech}^2 \left[\frac{1}{2} \sqrt{\frac{C}{\beta}} (x - c_0(1 - C)t) \right],$$

and stability was settled affirmatively some time ago (see [3], [6], [11]). In [8], Benjamin presented a degree-theoretic proof of existence of solitary waves corresponding to all values of γ in the range $0 \leq \gamma < 1$ (An alternative proof based on the Concentrated-Compactness Principle has been worked out in [15]). Benjamin also outlined an argument, based on the Implicit Function Theorem for proving existence of solitary waves when γ is small. The aim of this section is to complete and generalize the latter argument. Although limited to the case of small γ , it has several advantages over the degree-theoretic approach. First, it is constructive in nature, and leads naturally to the method used below in Section 4 to compute solitary waves numerically for all values of γ in $[0, 1)$. Secondly, the arguments used here yield not only the existence of a branch of solitary waves for an interval of positive values of γ , but also the continuity and in fact the analyticity of this branch with respect to γ . This in turn makes it possible to establish such properties as the stability of the solitary waves with regard to small perturbations of the wave profile, when considered as solutions of the time-dependent equation. In what follows, let $H^r(\mathbb{R})$ be the Sobolev space of functions q which satisfy

$$\|q\|_r^2 = \int_{\mathbb{R}} (1 + k^2)^r |\hat{q}(k)|^2 dk < \infty.$$

For any pair of Banach spaces X and Y , let $B(X, Y)$ be the space of bounded operators from X to Y with the operator norm.

Consider a general class of equations of the form

$$(10) \quad u_t + (f(u) + lg(u))_x - (M + lS)u_x = 0,$$

where $f : \mathbb{R} \rightarrow \mathbb{R}$, $g : \mathbb{R} \rightarrow \mathbb{R}$, and M and S are Fourier multiplier operators defined by

$$\widehat{Mv}(k) = \rho(k)\hat{v}(k)$$

and

$$\widehat{Sv}(k) = \sigma(k)\hat{v}(k).$$

We make the following assumptions.

- (A1) The functions $\rho(k)$ and $\sigma(k)$ are measurable and even, and $\rho(k)$ is non-negative.
- (A2) There exists a number $s \geq 0$ and positive constants B_1 , B_2 , and B_3 such that, for all sufficiently large values of k , $B_1|k|^s \leq \rho(k) \leq B_2|k|^s$ and $|\sigma(k)| \leq B_3|k|^s$.
- (A3) The functions f and g are smooth, and $f(0) = g(0) = 0$.

A solitary-wave solution of Eq. (10) is a solution of the form $\bar{u}(x, t) = \Phi(x - Ct)$, where $C > 0$ is the wave speed and Φ is a localized function, which is to say that $\Phi(y) \rightarrow 0$ as $y \rightarrow \pm\infty$ at least at an algebraic rate. We say that such a solution is (orbitally) stable, with respect to a given norm, if the distance between a solution $u(x, t)$ of Eq. (10) and the orbit $\{\bar{u}(\cdot, t) : t \geq 0\}$ remains arbitrarily small in norm for all time, provided only that $u(x, 0)$ is close enough in norm to $\bar{u}(x, 0)$.

The present-day theory of stability of solitary waves dates back to the paper of Benjamin [6] as corrected in [11], and has undergone considerable development since then (cf. [3], [13], [18], [27]). Here we employ the criterion for stability set forth in [13]. Define the operator $\mathcal{L} : L^2(\mathbb{R}) \rightarrow L^2(\mathbb{R})$ by

$$(11) \quad \mathcal{L} = C + M + lS - f'(\Phi) - lg'(\Phi),$$

where C , $f'(\Phi)$, and $g'(\Phi)$, are viewed as multiplication operators. According to Theorem 4.1 and the proof of Lemma 5.1 of [13], the solitary wave $\bar{u}(x, t) = \Phi(x - Ct)$ will be stable with respect to the $H^{s/2}$ -Sobolev norm provided that the following two conditions on \mathcal{L} are met:

- (C1) when viewed as an operator on $L^2(\mathbb{R})$ with domain H^s , \mathcal{L} is self-adjoint, with one simple negative eigenvalue, a simple eigenvalue at zero, and no other part of its spectrum on the non-positive real axis, and
- (C2) there exists $\chi \in L^2(\mathbb{R})$ such that $\mathcal{L}(\chi) = \Phi$ and $\int_{-\infty}^{\infty} \chi(x)\Phi(x) dx < 0$.

We now make a final assumption about Eq. (10).

- (A4) For $l = 0$, Eq. (10) has a solitary-wave solution $u(x, t) = \Phi_0(x - Ct)$, where $C > 0$ and $\Phi_0(x)$ is a smooth, even function which belongs, together with all its derivatives, to the space $L^2(\mathbb{R})$. Moreover, the operator \mathcal{L}_0 associated to Φ_0 via Eq. (11) satisfies conditions (C1) and (C2) above.

It will now be shown that assumptions (A1) through (A4) imply the existence of an analytic map $l \mapsto \Phi_l$, defined for l in a neighborhood of $l = 0$ and taking values in $L^2(\mathbb{R})$, such that for each l , the function $u(x, t) = \Phi_l(x - Ct)$ is a stable, solitary-wave solution of Eq. (10). The proof of this assertion proceeds via the Implicit Function Theorem and relies on the classical perturbation theory of linear operators as expounded in Kato's book [21]. It is straightforward in outline, but not all the details are simple.

For $r > 0$, let H_e^r denote the closed subspace of all even functions in $H^r(\mathbb{R})$. From assumption (A2) it follows that there exist positive constants l_1 , B_4 and B_5 such that for all $l \in (-l_1, l_1)$ and for $|k|$ sufficiently large, one has

$$(12) \quad B_4(1 + k^2)^{s/2} \leq C + \rho(k) + l\sigma(k) \leq B_5(1 + k^2)^{s/2}.$$

In consequence, the function $C + \rho(k) + l\sigma(k)$ defines a multiplication operator \mathcal{M} on the space $\{\hat{q} : q \in H_e^1\}$ whose maximal domain is the space $\{\hat{q} : q \in H_e^{1+s}\}$. Since maximal multiplication operators are self-adjoint, and the operator $C + M + lS$ is unitarily equivalent to \mathcal{M} via the Fourier transform, then $C + M + lS$ is self-adjoint on H_e^1 with domain H_e^{1+s} . It is straightforward to adduce that for small enough l , the spectrum of the operator \mathcal{M} , and hence the operator $C + M + lS$, is a subset of an interval of the form $[b, +\infty)$, $b > 0$, and is comprised of continuous spectrum.

Let ϕ denote any function in H_e^1 , and define the multiplication operator Q on H_e^1 by $Q\psi = (f'(\phi) + lg'(\phi))\psi$. Since $f'(\phi) \in H_e^1$, $g'(\phi) \in H_e^1$, and H_e^1 is an algebra, it follows that Q is a bounded operator on H_e^1 . Hence, by Theorem V-4.3 of [21], the

operator $C + M + lS - Q$ is self-adjoint on H_e^1 with domain H_e^{1+s} . Moreover, Q is relatively compact with respect to $C + M + lS$ (this may be verified, for example, by using the argument in the proof of Lemma 3.17 of [4] together with the fact that

$$\int_{|x| \geq R} |f'(\phi) + lg'(\phi)|^2 dx \quad \text{and} \quad \int_{|x| \geq R} |((f'(\phi))' + lg'(\phi))'|^2 dx$$

tend to zero as $R \rightarrow \infty$). Hence, as in Theorem V-5.7 of [21], it follows that the spectrum of \mathcal{L} consists of a continuous spectrum, identical to that of $C + M + lS$, together with a finite number of real eigenvalues of finite multiplicity.

Let $I = (-l_1, l_1)$, and define a map $F : I \times H_e^{1+s} \rightarrow H_e^1$ by

$$F(l, \phi) = (C + M + lS)(\phi) - f(\phi) - lg(\phi).$$

A calculation shows that the Fréchet derivative $F_\phi = \frac{\delta F}{\delta \phi}$ exists on $I \times H_e^{1+s}$ and is defined as a map from $I \times H_e^{1+s}$ to $B(H_e^{1+s}, H_e^1)$ by

$$F_\phi(l, \phi) = C + M + lS - Q.$$

From hypothesis (A4), it follows that $F(0, \Phi_0) = 0$ and that the operator $\mathcal{L}_0 = F_\Phi(0, \Phi_0)$ has a one-dimensional nullspace N in $L^2(\mathbb{R})$. Upon substituting $u(x, t) = \Phi_0(x - Ct)$ in Eq. (10) and differentiating once with respect to x , one finds that $\mathcal{L}_0(\Phi_0') = 0$, whence $\Phi_0' \in N$. Since Φ_0' is odd, it is not a member of H_e^{1+s} , and it follows that $\mathcal{L}_0 : H_e^{1+s} \rightarrow H_e^1$ is invertible. Finally, since L and M map H_e^{1+s} into H_e^1 boundedly and the maps $\phi \mapsto f(\phi) + lg(\phi)$ and $\phi \mapsto f'(\phi) + lg'(\phi)$ are continuous maps from H_e^1 into itself, then F and F_ϕ are continuous maps from $I \times H_e^{1+s}$ into their respective target spaces H_e^1 and $B(H_e^{1+s}, H_e^1)$. Hence all the conditions of the Implicit Function Theorem (see [17], Theorem 15.1) are met, and it may be concluded that there exist a number $l_2 > 0$ and a continuous map $l \mapsto \Phi_l$ from $(-l_2, l_2)$ to H_e^{1+s} such that $F(l, \Phi_l) = 0$ for all $l \in (-l_2, l_2)$. Indeed, since $F(l, \Phi)$ depends analytically on l , the map $l \mapsto \Phi_l$ is analytic as well.

The existence of the desired family of solitary-wave solutions of Eq. (10) has now been demonstrated, and it remains to prove that these solitary waves are stable, at least when l is sufficiently near zero. Consider the map

$$l \mapsto \mathcal{L}_l = F_\Phi(l, \Phi_l),$$

which is defined on the interval $(-l_2, l_2)$ and takes values in the space \mathcal{C} of closed operators on $L^2(\mathbb{R})$. For l, l' in $(-l_2, l_2)$, it follows from Eq. (12) that

$$\begin{aligned} \|(C + M + lS)^{-1} - (C + M + l'S)^{-1}\|_{B(L^2, L^2)} &= \\ \sup_{k \in \mathbb{R}} |(C + \rho(k) + l\sigma(k))^{-1} - (C + \rho(k) + l'\sigma(k))^{-1}| & \\ \leq |l - l'| \sup_{k \in \mathbb{R}} \left(\frac{(B_5/l_1)(1 + k^2)^{s/2}}{B_4(1 + k^2)^s} \right). & \end{aligned}$$

Hence $(C + M + lS)^{-1}$ tends to $(C + M + l'S)^{-1}$ in the norm of the space of bounded operators on $L^2(\mathbb{R})$ as l approaches l' . Therefore, by Theorems IV-2.14 and IV-2.20 of [21], \mathcal{L}_l varies continuously with l in the topology of generalized convergence on \mathcal{C} . Hence the results of section IV-4 of [21] imply that the eigenvalues of \mathcal{L}_l depend continuously on l . In particular, since the function Φ_l' is an eigenfunction of \mathcal{L}_l with eigenvalue 0, one obtains that the condition (C1) holds for all l sufficiently near zero. Also, for these values of l , 0 is not an eigenvalue of \mathcal{L}_l in H_e^1 , and therefore by Theorem

IV-2.25 of [21], the operator \mathcal{L}_l^{-1} varies continuously with l in $B(L_e^2, L_e^2)$. Hence the map $l \mapsto \mathcal{L}_l^{-1}(\Phi_l)$ is a continuous L_e^2 -valued map for l in some neighborhood of zero, and so the condition (C2) holds for these values of l . This is enough to conclude, by the theory put forward in [13], that the corresponding solitary waves Φ_l are stable.

To apply the above theory to the Benjamin equation, first make the change of variables $u(x, t) = \eta(x - t, -t/c_0)$, reducing Eq. (1) to

$$u_t - 2ruu_x + \alpha Lu_x + \beta u_{xxx} = 0,$$

which has the form of Eq. (10) with $f(u) = -ru^2$, $g(u) = 0$, $\rho(k) = \beta k^2$, $\sigma(k) = -|k|$, and $l = \alpha$. Assumptions (A1) through (A3) clearly hold in this case; and assumption (A4) becomes a well-known property of the Schrödinger operator associated with the KdV-solitary wave (see [23]). Hence, from the general result just expounded, it follows that for every $C > 0$ there exists a number $\alpha_0 = \alpha_0(C)$ such that, for all $\alpha \in (-\alpha_0, \alpha_0)$, the above equation has a stable solitary-wave solution $u(x, t) = \Phi(x - Ct)$. Then $\eta(x, t) = \Phi(x - c_0(1 - C)t)$ is a stable solitary-wave solution to Eq. (1). In fact, using the transformation in Eq. (4) one sees easily that the properties of existence and stability of solitary-wave solutions of Eq. (1) depend only on $\gamma = \alpha/2\sqrt{\beta C}$, in the sense that if $\alpha_1/2\sqrt{\beta_1 C} = \alpha_2/2\sqrt{\beta_2 C}$, then the profile function Φ_1 of a stable solitary-wave solution corresponding to α_1, β_1, C_1 is transformed via

$$\frac{1}{C_1} \Phi_1\left(\sqrt{\frac{\beta_1}{C_1}} X\right) = \frac{1}{C_2} \Phi_2\left(\sqrt{\frac{\beta_2}{C_2}} X\right)$$

into the profile function Φ_2 of a stable solitary-wave solution corresponding to α_2, β_2, C_2 . Hence the number α_0 defined above can be taken as $\alpha_0 = 2\gamma_0\sqrt{\beta C}$, where γ_0 is independent of C .

It is also known (see [1], [10]) that assumptions (A1) through (A4) are valid if one takes $\rho(k) = |k|$ (so that Eq. (10) with $l = 0$ is the Benjamin-Ono equation) or if $\rho(k) = k \coth kh - (1/h)$, where $h > 0$ (in which case Eq. (10) with $l = 0$ is known as the Intermediate Long-Wave equation). Therefore the above theory applies, and one may conclude that existence and stability of solitary waves persists for perturbations of these equations as well.

4 NUMERICAL APPROXIMATION OF SOLITARY WAVES

4.1 Description of the Numerical Scheme.

Solitary-wave solutions of Eq. (5), rescaled via the transformation $X \rightarrow \lambda X$, where λ is a spatial scaling factor, will be approximated by parameter-continuation methods. The scaling factor is used to dilate or contract the support of the computed solution over a fixed computational interval. An increase in the value of the scaling factor makes the significant support of the solution larger as compared to the computational interval. In the examples presented in this study, $\lambda = 0.051$.

A family of solutions to Eq. (5) for $\gamma \in [0, 1)$ on $X \in [0, 2\pi]$ was found numerically by using a continuation-method strategy. Some of these calculated approximations appear in Figures 3 and 4. These figures indicate that the solitary-wave solutions are symmetric waves which have prominent oscillatory tails when γ is close to 1, and, for a fixed value of the wave-speed c , whose maximum excursion from the rest state decreases as the parameter γ approaches 1 (see Figure 5).

To solve Eq. (5), the nonlinear differential equation is first recast as a system of algebraic equations using Fourier methods. For an even, positive integer N , denote

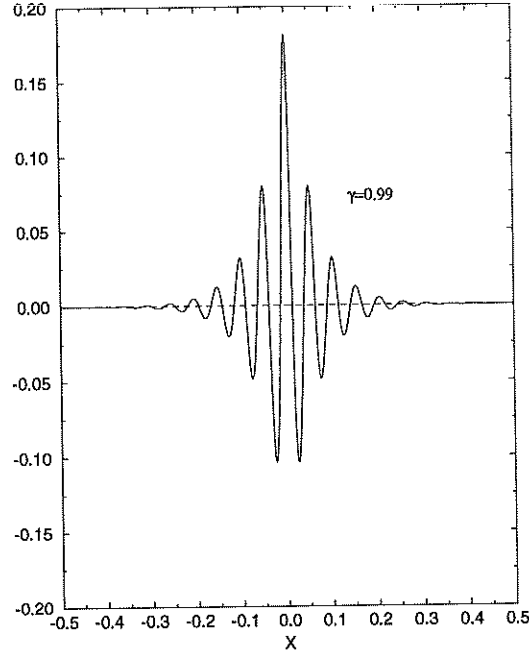


FIGURE 4. Solitary-wave solution for $\gamma = 0.99$. The spatial domain has been scaled to unity. Note the vertical scale. $N = 512$.

$I_N \phi \in S_N$ denote the trigonometric interpolant of the function ϕ at the points X_j , where $X_j = j2\pi/N$, $0 \leq j < N$. That is, $I_N \phi$ is the unique element of S_N that agrees with ϕ at $X = X_j$, $0 \leq j < N$. Then, as is well-known [14], the bound on the interpolation error is

$$(13) \quad \|\phi - I_N \phi\|_{L^2(\mathbb{T})} \leq C_I (N/2)^{-s} \left\| \frac{\partial^s \phi}{\partial X^s} \right\|_{L^2(\mathbb{T})},$$

where C_I is a constant. The inequality in Eq. (13) is valid for all $\phi \in H_p^s(\mathbb{T})$, the periodic subspace of the Sobolev space of order s on $[0, 2\pi]$, defined as the set of all $f \in L^2(\mathbb{T})$ such that $\sum_{k \in \mathbb{Z}} |k|^{2s} |\hat{f}(k)|^2 < \infty$.

Demanding that the operator Q applied to the interpolation $I_N \phi$ have zero projection in S_N , which is to say $(\hat{Q}(I_N \phi, \gamma), \psi(k))_{L_2} = 0$ for $-N/2 \leq k < N/2$, yields the system of equations

$$c(k; \gamma) \hat{\phi}(k) - (\hat{\phi} * \hat{\phi})(k) = 0$$

for the Fourier coefficients of ϕ . Here, $c(k; \gamma) = 1 - 2\gamma|k|\lambda + \lambda^2 k^2$ and the discrete convolution in the second term is defined as the sum $(\hat{\phi} * \hat{\phi})(k) = \sum_l \hat{\phi}(l) \hat{\phi}(k-l)$, with $-N/2 \leq l < N/2$. The above nonlinear system may be written compactly as the one-parameter system

$$(14) \quad Y(\gamma, \hat{\phi}(k)) = 0,$$

where $Y : [0, 1] \times \mathbb{C}^N \rightarrow \mathbb{C}^N$. For a fixed value of γ , the approximate solution ϕ is given by the inverse discrete Fourier transform of the Fourier coefficients $\{\hat{\phi}\}_{k=-N/2}^{N/2-1}$ which are the solution of Eq. (14). Assuming Eq. (14) has a branch of solutions that is continuously differentiable with respect to the parameter γ , homotopy methods [25, pp. 127–129] present a potentially useful method for determining this branch. The method uses a known solution corresponding to a particular value of γ as an initial

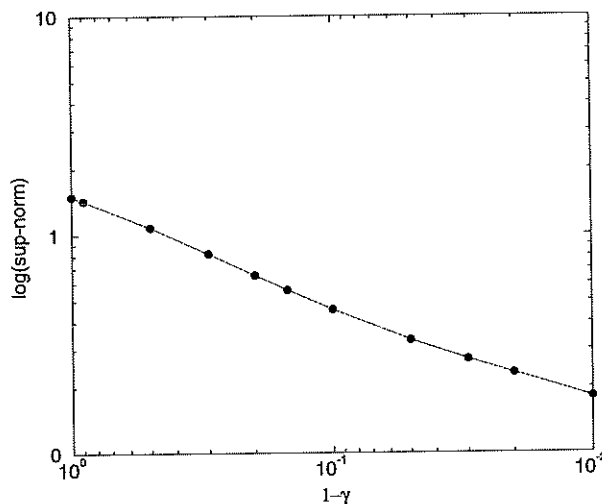


FIGURE 5. *Logarithm of the sup-norm of the computed solutions as a function of $1 - \gamma$. $N = 512$.*

guess in an iterative procedure which seeks to compute a nearby solution on the branch with a slightly different value of γ . This strategy is bound to succeed if the branch of solutions does not feature bifurcations or folds. In the case of Eq. (14), a solution is known for $\gamma = 0$, namely the projection onto S_N of the solitary-wave solution to the KdV equation, and thus it is possible to initiate a parameter-continuation search of approximations to an entire branch of solutions to Eq. (5) for $0 \leq \gamma < 1$. We proceed now to a description of the specific implementation of the general idea just enunciated.

Numerically, Eq. (14) is approximated by elements $\phi(\cdot, \gamma) \in S_N$ such that

$$(15) \quad \|Y(\gamma, \hat{\phi}(k, \gamma))\|_{l_2} < r,$$

where l_2 is the space of square-summable sequences and the residual r was taken to be 10^{-13} for all cases reported in this study. Several values $\gamma_j^* \in [0, 1)$ are chosen for which the solutions $\phi(X, \gamma_j^*)$ are desired. The set is arranged so that $\gamma_{j+1}^* > \gamma_j^*$ and $\gamma_0^* = 0$. The set $\{\gamma_j^*\}_{j=1}^J$ used in this report is listed in Table 1. Each segment $[\gamma_j^*, \gamma_{j+1}^*]$ is divided into M_m equal segments of size $\Delta_m = 2^{-m}\Delta$, where Δ is a number that is much smaller than the segment's length and is commensurate with it. The refinement level is characterized by $m = 0, 1, 2, \dots$. The discrete values of the parameter in the segment depend on the refinement level and are given by

$$\gamma^n = \gamma_j^* + n\Delta_m, \quad \text{for } n = 0, 1, \dots, M_m.$$

The Newton-Raphson method is used to find an approximation $\hat{\phi}(k, \gamma^{n+1})$ from $\hat{\phi}(k, \gamma^n)$. This requires the solution of the system of equations

$$(16) \quad \mathbf{J}^n \hat{\phi}(k, \gamma^{n+1}) = \mathbf{J}^n \hat{\phi}(k, \gamma^n) - \mathbf{A}^n (\gamma^{n+1} - \gamma^n), \quad -N/2 \leq k < N/2,$$

for $\hat{\phi}(\cdot, \gamma)$, where $\mathbf{J}^n = \partial Y^i / \partial \hat{\phi}(k, \gamma^n)$ and $\mathbf{A}^n = \partial Y^i / \partial \gamma^n$, $-N/2 \leq i < N/2$. When $n = M_m$, so that $\gamma^{M_m} = \gamma_{j+1}^*$, the set of $\hat{\phi}$ calculated with parameter step size Δ_m is compared to the previously computed solution, obtained with parameter step size

Δ_{m-1} . This comparison is subjected to the test

$$(17) \quad \|\hat{\phi}^m(k, \gamma_{j+1}^*) - \hat{\phi}^{m-1}(k, \gamma_{j+1}^*)\|_{l_2} < \epsilon,$$

where the tolerance ϵ was set to 10^{-11} in all the examples appearing in this study. Obviously, Eq. (17) is not checked for $m = 0$. If, for a given m , the condition in Eq. (17) fails, the parameter step size is set to Δ_{m+1} , leading to a new value M_{m+1} , and the whole process is started over setting $\hat{\phi}^{m+1}(k, \gamma^{n=0}) = \hat{\phi}(k, \gamma_j^*)$. The entire calculation is started using the analytic solution $\hat{\phi}(k) = \frac{3}{2} \text{sech}^2(X/2)$ corresponding to $\gamma_0^* = 0$.

4.2 Numerical Results.

The calculations were performed using double-precision arithmetic on a DEC-Alpha 3000 machine. Real cosine Fourier transforms were used to effect the construction of the system in Eq. (14) since real even solutions were sought. The Jacobian matrix was calculated by hand. The solution of Eq. (16) was found by using standard LINPACK solvers. The nonlinear terms were evaluated pseudo-spectrally; that is, instead of performing the convolution, the nonlinear term was calculated in real space. As is clear from Figure 7, the spectrum of the solution is quite compact even for small values of λ . Thus, aliasing was not difficult to circumvent, provided sufficiently many Fourier components were used. The iteration history for a full range of γ for $N = 256$, shown in Table 1, attests to the good convergence characteristics of the Newton-Raphson solver used throughout the calculation. Values of Δ_m that achieved the required tolerances in reaching each γ_j^* are listed in Table 1. The homotopy stage between $\gamma = 0.8$ and $\gamma = 0.9$ required the smallest values of Δ_m to obtain good accuracy. The residual column shows the approximately-quadratic convergence rate of the Newton Raphson stage of the calculation at those particular values of Δ_m .

The Jacobian \mathbf{J} of Y is invertible, at least for small values of γ . We found in the calculations no evidence of folds or bifurcations on the branch of solutions corresponding to $\gamma \in [0, 1)$. We monitored the condition number of the Jacobian each time it was assembled in the Newton-Raphson procedure. The condition number decreased as γ increased and depended on N . Its value was more sensitive to N than γ , and was on the order of 10^{-1} to 10^{-3} for $N = 32$ and $N = 512$, respectively. The condition number was certainly small, but the accuracy of our calculations was such that we could safely assert it to be non-zero throughout our computations. A plot of the l_2 -norm of the solution as a function of the parameter γ (see Figure 6) offers no indication of branching of solutions. (The figure is actually a superposition of the graphs produced with $N = 64, 128, 256$, and 512 Fourier interpolants, and, as is evident, for any value of γ , the l_2 -norm was substantially the same regardless of N .)

The value of the invariants F and G defined in Section 1 (see below (1)), when evaluated on an approximation to a solitary-wave solution, are listed as a function of the number of interpolants for several values of γ in tables 2 and 3. It is noted that the invariants do not change in value with N for $N \geq 128$. For the values of γ discussed here, it was found that $N = 128$ was more than adequate to approximate solutions ϕ of Benjamin's equation with tolerances $\epsilon = 10^{-11}$ and $r = 10^{-13}$. Note that the Hamiltonian $F + G$ is positive in the range of γ considered here. The Hamiltonian decreases with γ , reaching very small values as γ approaches 1.

The key to resolving these particular wave profiles is capturing the peak in the Fourier spectra that results from the competition of the dispersion associated with α and the dispersion associated with β . As shown in Figure 7, the bandwidth of the

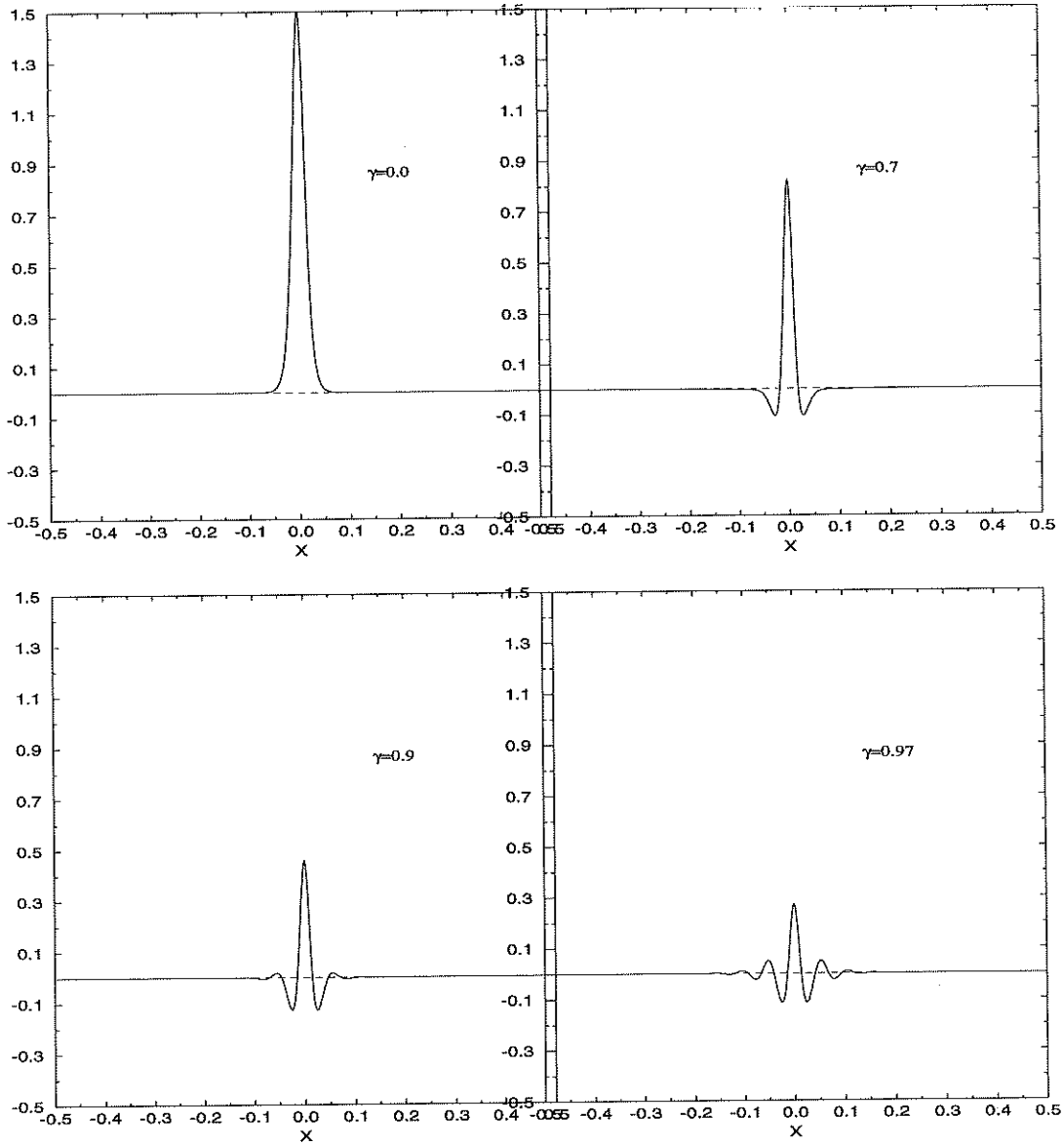


FIGURE 3. Solitary-wave solutions, scaled to the domain $[-0.5, 0.5]$. (a) $\gamma = 0.00$, (b) $\gamma = 0.70$, (c) $\gamma = 0.90$, (d) $\gamma = 0.97$. The vertical scale is the same in all figures. $N = 512$.

by S_N the space of trigonometric polynomials of degree up to $N/2$, which is to say

$$S_N = \text{span}\{e^{ikX} \mid -N/2 \leq k < N/2\}.$$

Let $P_N : L^2(\mathbb{T}) \rightarrow S_N$ be the orthogonal projection on S_N in the standard inner product (\cdot, \cdot) of $L^2(\mathbb{T})$ where $\mathbb{T} = [0, 2\pi]$. Thus, $P_N\phi$ is the truncated Fourier series

$$P_N \left[\sum_{k=-\infty}^{\infty} \hat{\phi}(k)\psi(k) \right] = \sum_{k=-N/2}^{N/2-1} \hat{\phi}(k)\psi(k)$$

of ϕ , where $\psi(k) = e^{ikX}$ and $\hat{\phi}(k)$ denotes the k^{th} Fourier coefficient of ϕ . Let

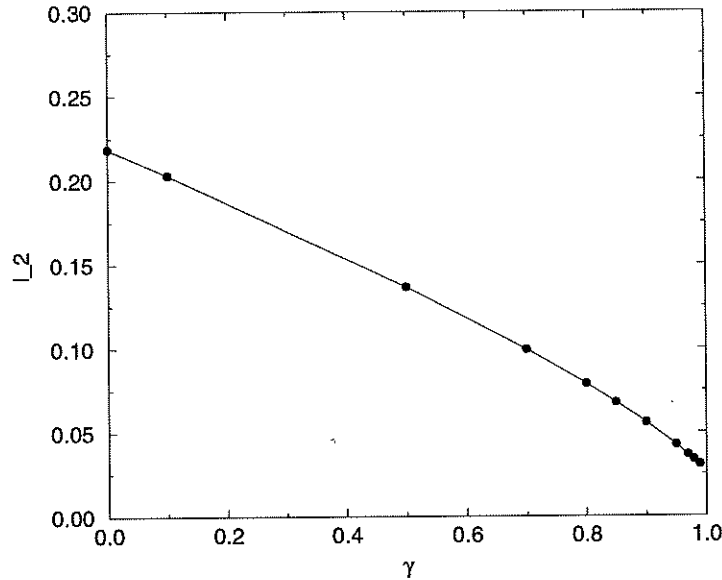


FIGURE 6. The l_2 -norm of the solution versus γ . The superposition of the norms computed with $N = 64, 128, 256, 512$ Fourier interpolants are indistinguishable.

spectra with significant energy is approximately $0 \leq |k| \leq 60$. Attempting to resolve the wave with a smaller bandwidth yields a solution with a qualitatively different shape. Figure 8 shows a portion of the spectrum $\hat{\phi}(k)$ computed using the algorithm outlined in Section 4.1 with $\gamma = 0.85$. The upper curve is the superposition of the spectra computed with $N = 64$, $N = 128$, and $N = 256$, respectively. It was found that the spectra for $N > 64$ superimposes rather well on the $N = 64$ case. The lower curve represents the spectrum as computed using $N = 32$ and clearly does not capture the characteristic peak in the wave's spectrum. The example in this figure corresponds to $\gamma = 0.85$. Not surprisingly, the $N = 32$ case did not meet the tolerance associated with the parameter ϵ . To come to the approximation whose spectrum is displayed in Figure 8 using $N = 32$, this criteria had to be relaxed from $\epsilon = 10^{-11}$ to $\epsilon = 10^{-5}$.

Figure 9 shows the energetic portion of the Fourier spectra $\hat{\phi}(k)$ for several values of γ , making it clear that the peak of the spectrum moves to higher modes as γ gets larger, and the morphology of the spectrum changes significantly in the region adjoining the peak for γ near 1. Furthermore, from the same figure it is evident that, at $k = 0$, the spectrum $\hat{\phi}(k)$ has a non-zero right-hand derivative. Since $\hat{\phi}(k)$ is an even function in k , it follows that there is a discontinuity in the spectrum at $k = 0$. Consideration of the symbol $c(k)$ suggests that this should indeed be the case for all $\gamma \neq 0$. In this respect, the Fourier transform of the solitary waves discussed here resembles the explicit spectral function $\hat{\phi}(k) = \pi e^{-|k|}$ of the solitary-wave solution $\phi(X) = \frac{1}{1+X^2}$ of the Benjamin-Ono equation.

In [8] Benjamin derived a formal asymptotic estimate for $\phi(X)$ for large X . For γ near 1, he obtained

$$(18) \quad \phi(X) \sim -4K\gamma/X^2 + \frac{2\pi}{1-\gamma^2} |f(y_1)| \exp(-\sqrt{1-\gamma^2}X) \cos[\gamma X + \arg(f(y_1))]$$

as $X \rightarrow \infty$, where K is a constant and f is a function of the pole $y_1 = \gamma + i\sqrt{1-\gamma^2}$

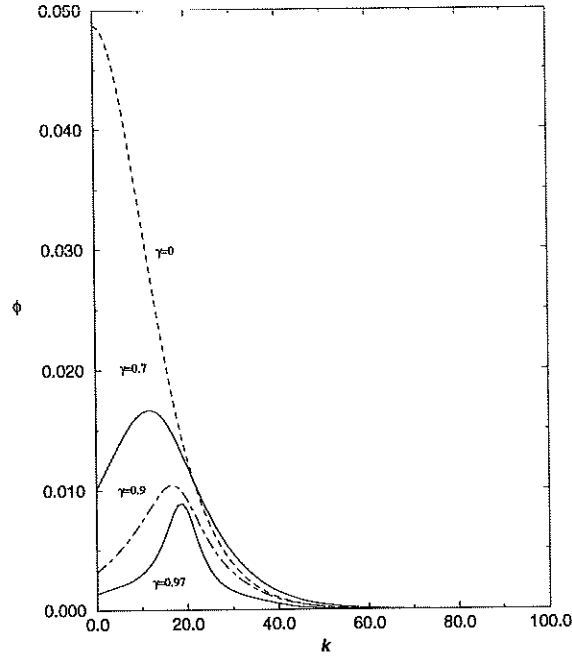


FIGURE 7. Portion of the Fourier spectra as a function of γ . $N = 512$.

TABLE 1

Residuals in reaching γ^* in the Newton-Raphson stage of the $N = 256$ run. The Δ_m 's quoted in the table correspond to the size of the step employed to reach γ_j^* within the error tolerances. Tolerance on the residual was 10^{-13} .

| γ^* | Δ_m | Residual | γ^* | Δ_m | Residual |
|------------|------------|--------------|------------|------------|--------------|
| 0.10 | 3.125E-03 | 4.274742E-05 | 0.80 | 1.250E-02 | 1.353319E-05 |
| | | 5.171706E-08 | | | 7.966373E-08 |
| | | 1.806914E-13 | | | 7.479083E-12 |
| | | 5.877141E-25 | | | 5.099222E-20 |
| 0.20 | 5.000E-02 | 4.808639E-05 | 0.90 | 9.766E-05 | 1.689451E-05 |
| | | 7.438409E-08 | | | 3.287065E-07 |
| | | 4.198945E-13 | | | 4.811537E-10 |
| | | 4.044869E-24 | | | 1.057499E-15 |
| 0.30 | 2.500E-02 | 1.159375E-05 | 0.95 | 1.250E-02 | 3.065973E-22 |
| | | 5.338055E-09 | | | 1.236640E-34 |
| | | 2.623204E-15 | | | |
| | | | | | |
| 0.40 | 2.500E-02 | 1.100423E-05 | 0.97 | 6.250E-03 | 1.286097E-27 |
| | | 6.216201E-09 | | | 4.376426E-35 |
| | | 4.582266E-15 | | | |
| | | | | | |
| 0.50 | 2.500E-02 | 4.157460E-05 | 0.98 | 6.250E-03 | 1.645986E-31 |
| | | 1.100305E-07 | | | 7.247277E-36 |
| | | 1.945366E-12 | | | |
| | | 2.833418E-22 | | | |
| 0.70 | 2.500E-02 | 3.180455E-05 | 0.99 | 6.250E-03 | 3.356281E-15 |
| | | 1.664470E-07 | | | 1.798301E-24 |
| | | 1.296935E-11 | | | |
| | | 5.133442E-20 | | | |

TABLE 2
F as a function of the number of interpolants.

| γ | 64 | 128 | 256 | 512 |
|----------|--------------|--------------|--------------|--------------|
| 0.00 | 2.435081E-02 | 2.435071E-02 | 2.435071E-02 | 2.435071E-02 |
| 0.10 | 2.102588E-02 | 2.103165E-02 | 2.103165E-02 | 2.103165E-02 |
| 0.50 | 9.506347E-03 | 9.521296E-03 | 9.521296E-03 | 9.521296E-03 |
| 0.70 | 5.015357E-03 | 5.029482E-03 | 5.029482E-03 | 5.029482E-03 |
| 0.90 | 1.578698E-03 | 1.583581E-03 | 1.583581E-03 | 1.583581E-03 |
| 0.99 | 4.785824E-04 | 4.790875E-04 | 4.790875E-04 | 4.790875E-04 |

TABLE 3
G as a function of the number of interpolants.

| γ | 64 | 128 | 256 | 512 |
|----------|---------------|---------------|---------------|---------------|
| 0.00 | 2.435218E-02 | 2.435071E-02 | 2.435071E-02 | 2.435071E-02 |
| 0.10 | 1.944642E-02 | 1.944358E-02 | 1.944358E-02 | 1.944358E-02 |
| 0.50 | 4.398194E-03 | 4.391453E-03 | 4.391454E-03 | 4.391454E-03 |
| 0.70 | 4.140576E-04 | 4.068088E-04 | 4.068088E-04 | 4.068088E-04 |
| 0.90 | -7.622961E-04 | -7.658048E-04 | -7.658048E-04 | -7.658048E-04 |
| 0.99 | -4.403099E-04 | -4.407939E-04 | -4.407939E-04 | -4.407939E-04 |

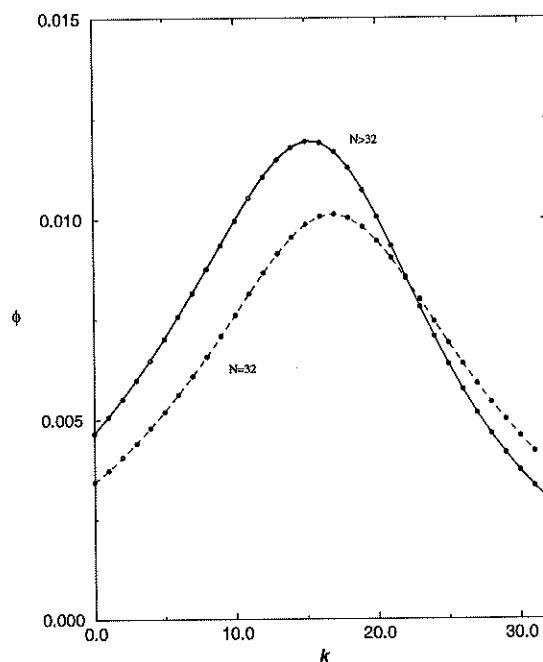


FIGURE 8. *Fourier spectra of the solution for $\gamma = 0.85$. The lower curve corresponds to the $N = 32$ case, while the upper curve was computed using $N = 64$, $N = 128$, and $N = 256$. Dots show the location of the calculated discrete spectral points.*

of $1/(1 - 2\gamma|k| + k^2)$. The second term on the right-hand side of the above expression decays exponentially as $X \rightarrow \infty$, whereas the first term decays only algebraically, so that for very large values of X , the first term will dominate the second. As γ approaches 1, however, the coefficient $2\pi/(1 - \gamma^2)$ of the second term will be much larger than the coefficient of the first term, while the factor of $\sqrt{1 - \gamma^2}$ within the exponential will become small, so that the second term will dominate the first term over

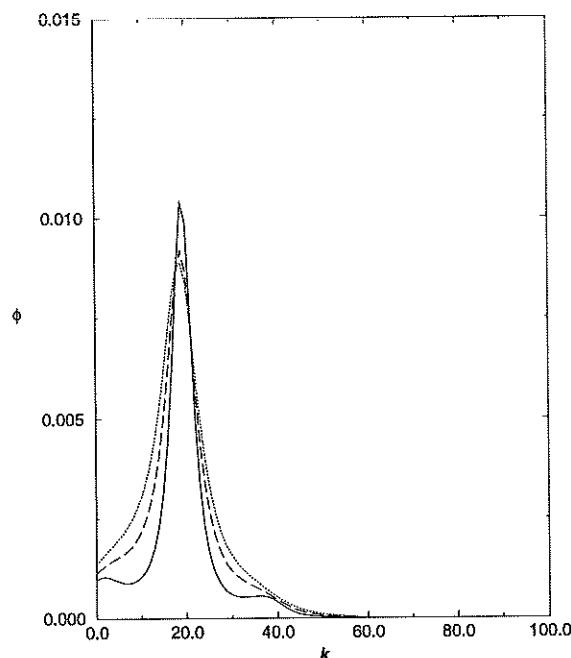


FIGURE 9. Portion of the spectra as a function of γ , $N = 512$. Solid: $\gamma = 0.99$, dashed: $\gamma = 0.98$, dotted: $\gamma = 0.97$.

an ever-increasing range of values of X . Within this range, according to Benjamin's asymptotic expression (18), the zeros of $\phi(X)$ will be near the zeros of $\cos(\gamma X)$, and hence will be spaced at intervals of length approximately π/γ .

Our numerical approximations of $\phi(X)$ conform to the above predictions. Figures 3 and 4 show that the range of values of X over which $\phi(X)$ exhibits oscillatory behavior increases as γ approaches 1, and that within this range the zeros of $\phi(X)$ are fairly evenly spaced. To compare the spacing between the zeros with the value π/γ predicted by Benjamin's estimate, we considered an approximate solution $\phi(X) = \phi(X; \gamma)$ with $\gamma = 0.99$, computed with $N = 2048$. A total of 17 zeros were found on either side of the $X = 0$ axis. Since linear interpolation was used between the 2048 data points, the location of these zeros carries an uncertainty of approximately $\pm 2.44 \cdot 10^{-4}$. In the scaling used here, for $\gamma = 0.99$, Benjamin's estimate predicts a spacing between the zeros of $z^* = \lambda/2\gamma = 2.5758 \cdot 10^{-2}$. Table 4 lists the location Z of the zeros and the intervals z between them for $X > 0$. The computed values of z show adequate agreement with z^* . Note that the deviation of z from z^* for the largest values of Z is consistent with Benjamin's estimate. Since the largest values of Z occur in a region where the two terms in the estimate are nearly in balance, one would not expect their spacing to be determined by the second term alone.

It deserves remark that the formal asymptotic derived in [8] and displayed in (18) is different from Benjamin's conclusion on the same topic in [7]. In the latter reference, Benjamin asserted the solitary-wave solutions of his equation decayed exponentially and oscillated infinitely often. Certainly, solitary-wave solutions ϕ of (1) cannot decay exponentially since then, by the Paley-Wiener Theorem, their Fourier transform $\hat{\phi}$ would be analytic, so infinitely differentiable, and indeed all its derivatives would lie in $L^2(\mathbb{R})$. This conclusion is not compatible with the singular aspect of the dispersion c_B in (3). The matter has been rigorously settled in a recent paper of Chen and Bona

TABLE 4

Location of the zeros of $\phi(X, \gamma)$ with $\gamma = 0.99$, computed using $N = 2048$, displayed consecutively from left to right and top to bottom. The intervals between consecutive zeros, multiplied by 100, appear in parentheses.

| | | |
|------------------|------------------|------------------|
| 1.33E-02 (2.59) | 3.92E-02 (2.56) | 6.49E-02 (2.60) |
| 9.09E-02 (2.54) | 1.164E-01 (2.61) | 1.425E-01 (2.54) |
| 1.679E-01 (2.61) | 1.94E-01 (2.53) | 2.193E-01 (2.64) |
| 2.457E-01 (2.50) | 2.707E-01 (2.60) | 2.975E-01 (2.43) |
| 3.218E-01 (2.78) | 3.496E-01 (2.29) | 3.725E-01 (3.05) |
| 4.028E-01 (1.91) | 4.221E-01 | |

[15] using the decay results of Li and Bona [22], [12]. In [15], it is shown that

$$\lim_{x \rightarrow \pm\infty} X^2 \phi(X) = D,$$

where D is a non-zero constant. This is consistent with the formalism in (18) and implies that ϕ must feature at most finitely many oscillations.

5 CONCLUDING REMARKS

In this study, three themes were pursued in the context of Benjamin's equation for the approximation of internal waves in certain two-fluid systems where the effects of surface tension cannot be ignored. First, a reappraisal of the derivation of the equation is given with an eye toward better understanding the circumstances under which the equation might be expected to provide physically relevant information. Second, an exact analysis of solitary-wave solutions is provided via the Implicit Function Theorem. The analysis is so organized that information about the stability is also obtained. Finally, the Contraction Mapping Principle underlying the proof of existence of solitary waves is used as the basis of a continuation-type algorithm. This algorithm is implemented as a computer code which is used to obtain numerically generated approximations of these solitary waves.

Analysis of the Benjamin equation in its context as a model for waves in certain two-fluid systems reveals there are ranges of the physical parameters for which the model's predictions might be relevant to waves seen in the laboratory or natural settings. It must be acknowledged, however, that the range in question is somewhat narrow. As a next step, it would be useful to construct a reliable numerical scheme for the time-dependent problem (1)¹. The outcome of an organized set of simulations might well suggest aspects to look for in an experimental situation.

Previous experience with nonlinear, dispersive wave equations of the form depicted in (10) (with $l = 0$, say) indicates that solitary-wave solutions may play an important role in the long-time evolution of general disturbances. In consequence, we endeavored here to understand these traveling-wave solutions in some detail. The form of these solitary waves varies with the parameter $\gamma = \frac{1}{2}\alpha/\sqrt{C}\beta$, where C is the difference between the solitary-wave speed and the speed c_0 of infinitesimal waves of extreme length, and α and β are measures of the strengths of the competing dispersive effects (the parameter α is related to finite-depth effects whilst non-zero values of β are due to surface-tension effects). In a given setting, it is possible to cover the entire

¹ A time-dependent algorithm using a split-step method [20] based on Fourier projection for the linear terms alternated with a conservative second-order approximation for the advective terms is being developed.

range $0 < \gamma < 1$ by appropriate choices of the speed $c_0(1 - C)$ of the solitary wave. Values of γ near 0 correspond to traveling waves with large, negative phase velocities, however, and these lie outside the range where the equation is expected to be a valid model. Also, the results of Section 4 suggest that solitary waves corresponding to values of γ near 1 will have small amplitudes, making them hard to discern. When γ is order μ or greater, and is not too close to 1, the corresponding solitary waves travel to the right, and are potentially observable.

It is worth noting that the stability theory developed in Section 3 applies to the Benjamin equation only for values of γ near 0. The general stability theory for solitary-wave solutions of equations of the form depicted in (10) (cf. [2]) does not apply directly to the Benjamin equation. The problem of extending the stability theory to encompass the physically relevant regime is currently under study. In addition to an analytical approach, we expect to use the aforementioned computer code for approximating solutions of the time-dependent problem (1) to investigate stability via a coordinated set of numerical simulations with initial data corresponding to perturbed solitary waves.

The continuation method developed in Section 4 for the approximation of solitary-wave solutions of the Benjamin equation appears capable of producing traveling wave solutions over the entire range of γ . Another use of a time-dependent numerical integrator would be to check directly how closely the computed solitary waves correspond to traveling waves. Once this is settled satisfactorily, natural further questions include determining the outcome of interactions of solitary waves and whether or not general initial disturbances feature solitary waves in their long-time asymptotics. The results of Vanden-Broeck and Dias (cf. [26]) on a free-surface problem similar to the one considered here suggest that other branches of solitary-wave solutions to the Benjamin equation may exist besides the one on which our computed solutions lie. Numerical experiments like those described above may disclose whether such solutions exist and play a role in general solutions of the initial-value problem for the Benjamin equation.

REFERENCES

- [1] J. P. ALBERT, "Positivity properties and stability of solitary-wave solutions of model equations for long waves," *Comm. P.D.E.* 17 (1992), 1-22.
- [2] J. P. ALBERT & J. L. BONA, "Total positivity and the stability of internal waves in stratified fluids of finite depth," *IMA J. App. Math.* 46 (1991), 1-19.
- [3] J. P. ALBERT, J. L. BONA & D. HENRY, "Sufficient conditions for stability of solitary-wave solutions of model equations for long waves," *Phys. D* 24 (1987), 343-366.
- [4] J. P. ALBERT, J. L. BONA & J. -C. SAUT, "Model equations for stratified fluids," *Proc. Royal Soc. London, A* (1997).
- [5] T. B. BENJAMIN, "Internal waves of permanent form in fluids of great depth," *J. Fluid Mech.* 29 (1967), 559-592.
- [6] _____, "The stability of solitary waves," *Proc. Royal Soc. London, A* 328 (1972), 153-183.
- [7] _____, "A new kind of solitary wave," *J. Fluid Mechanics* 245 (1992), 401-411.
- [8] _____, "Solitary and periodic waves of a new kind," *Philos. Trans. Roy. Soc. London A* 354 (1996), 1775-1806.

- [9] T. B. BENJAMIN, J. L. BONA & D. K. BOSE, "Solitary-wave solutions of nonlinear problems," *Phil. Trans. Royal Soc. London, A* 340 (1990), 195–244.
- [10] D. P. BENNETT, R. W. BROWN, S. E. STANSFIELD, J. D. STROUGHAIR & J. L. BONA, "The stability of internal solitary waves," *Math. Proc. Cambridge Philos. Soc.* 94 (1983), 351–379.
- [11] J. L. BONA, "On the stability theory of solitary waves," *Proc. Royal Soc. London, A* 344 (1975), 363–374.
- [12] J. L. BONA & Y. A. LI, "Decay and analyticity of solitary waves," *J. Math. Pures Appliq.* (1997).
- [13] J. L. BONA, P. E. SOUGANIDIS & W. A. STRAUSS, "Stability and instability of solitary waves of Korteweg–de Vries type," *Proc. Royal Soc. London, A* 411 (1987), 395–412.
- [14] C. CANUTO, M. Y. HUSSAINI, A. QUARTERONI & T. A. ZANG, *Spectral Methods in Fluid Dynamics*, Springer-Verlag, New York–Heidelberg–Berlin, 1988.
- [15] H. CHEN & J. L. BONA, "Existence and asymptotic properties of solitary-wave solutions of Benjamin-type equations," submitted, 1997.
- [16] R. E. DAVIS & A. ACRIVOS, "Solitary internal waves in deep water," *Journal of Fluid Mechanics* 29 (1967), 593–616.
- [17] K. DEIMLING, *Nonlinear Functional Analysis*, Springer-Verlag, New York, 1985.
- [18] M. GRILLAKIS, J. SHATAH & W. STRAUSS, "Stability theory of solitary waves in the presence of symmetry, I," *J. Func. Anal.* 74 (1987), 160–197.
- [19] R. GRIMSHAW, "Evolution equations for long, nonlinear internal waves in stratified shear flows," *Stud. Appl. Math.* 65 (1981), 159–188.
- [20] A. HASEGAWA & F. TAPPERT, "Transmission of stationary nonlinear optical pulses in dispersive dielectric fibers. I. Anomalous dispersion," *Applied Physics Letters* 23 (1973), 142–144.
- [21] T. KATO, *Perturbation Theory of Linear Operators*, Springer-Verlag, New York, 1976.
- [22] Y. A. LI & J. L. BONA, "Analyticity of solitary-wave solutions of model equations for long waves," *SIAM J. Math. Anal.* 27 (1996), 725–737.
- [23] P. M. MORSE & H. FESHBACH, *Methods of Theoretical Physics, Vol 1*, McGraw-Hill, New York, 1953.
- [24] H. ONO, "Algebraic solitary waves in stratified fluids," *J. Phys. Soc. Japan* 39 (1975), 1082–1091.
- [25] R. SEYDEL, *Practical Bifurcation and Stability Analysis, from Equilibrium to Chaos*, IAM Series, Springer-Verlag, New York–Heidelberg–Berlin, 1994.
- [26] J. M. VANDEN-BROECK & F. DIAS, "Gravity-capillary solitary waves in water of infinite depth and related free-surface flows," *Journal of Fluid Mechanics* 240 (1992), 549–557.
- [27] M. WEINSTEIN, "Existence and dynamic stability of solitary-wave solutions of equations arising in long-wave propagation," *Comm. Partial Differential Equations* 12 (1987), 1133–1173.